

Probing Metabolism in the Intact Retina Using Stable Isotope Tracers

Jianhai Du^{*,†}, Jonathan D. Linton^{*,†}, James B. Hurley^{*,†,1}

^{*}Departments of Biochemistry, University of Washington, Seattle, Washington, USA

[†]Department of Ophthalmology, University of Washington, Seattle, Washington, USA

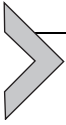
¹Corresponding author: e-mail address: jbh@u.washington.edu

Contents

1. Introduction	150
2. Methods	151
2.1 Choice of Stable Isotope Tracers and Labeling Method	152
2.2 Retinal Organ Culture	154
2.3 Retinal Organ Culture for Cryosection	155
2.4 Tracing Retinal Metabolism <i>In Vivo</i>	155
2.5 Sample Collection and Preparation	156
2.6 Analysis of Metabolites by GC-MS	159
2.7 Analysis of Metabolites by LC-MS	161
3. Applications	163
3.1 Neuron-Glia Interaction	163
3.2 Retinal Metabolism in Light and Dark Adaption	165
3.3 Retinal Degenerative Diseases	166
4. Summary	166
Acknowledgments	167
References	167

Abstract

Vertebrate retinas have several characteristics that make them particularly interesting from a metabolic perspective. The retinas have a highly laminated structure, high energy demands, and they share several metabolic features with tumors, such as a strong Warburg effect and abundant pyruvate kinase M2 isoform expression. The energy demands of retinas are both qualitatively and quantitatively different in light and darkness and metabolic dysfunction could cause retinal degeneration. Stable isotope-based metabolic analysis with mass spectrometry is a powerful tool to trace the dynamic metabolic reactions and reveal novel metabolic pathways within cells and between cells in retina. Here, we describe methods to quantify retinal metabolism in intact retinas and discuss applications of these methods to the understanding of neuron-glia interaction, light and dark adaptation, and retinal degenerative diseases.



1. INTRODUCTION

Vertebrate retinas are light-sensitive neural tissues with at least seven types of cells. Rods and cones are photoreceptors that detect light. Bipolar cells, horizontal cells, and amacrine cells are interneurons that process signals initiated by the photoreceptors. Ganglion cells relay the processed signals through the optic nerve to the brain (Dowling, 1970; Wassle & Boycott, 1991).

Photoreceptors, interneurons, and ganglion cells are confined to distinct layers in the retina. Müller glia radiate across all layers of the retina (Wassle & Boycott, 1991). Figure 1 illustrates structural features of the retina. Neurons and glia in the retina have a symbiotic relationship (Lindsay et al., 2014; Newman & Reichenbach, 1996). The laminated structure of the retina can be used to facilitate investigations of intracellular and intercellular metabolic pathways.

Nutrients enter the eye through blood vessels that enter the back of the eye along with the optic nerve. Blood flows into the choroid layer, which lines the inside surface of the sclera, the white part of the eye. Nutrients flow from the choroid layer, through the retinal pigment epithelial (RPE), through the interphotoreceptor matrix to the retina. In some retinas blood vessels on the inner surface of the retina or within the inner retina also provide a source of nutrients (Campbell & Humphries, 2012; Cunha-Vaz, Bernardes, & Lobo, 2011).

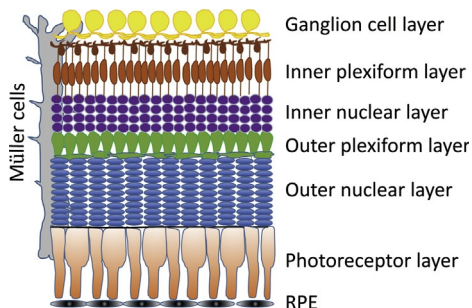


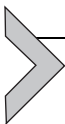
Figure 1 Laminar structure of vertebrate retina. The photoreceptor layer contains the outer segments and cell bodies of rods and cone cell bodies and the outer nuclear layer contains their nuclei; the inner nuclear layer contains nuclei of bipolar, amacrine, and horizontal and Müller cells; the inner plexiform layer contains dendrites and synapses of the inner retinal neurons and ganglion cells; the ganglion cell layer consists of ganglion cells; and Müller glia radiate across all layers of the retina. RPE is the retinal pigment epithelium.

Retinas have extraordinarily high energy demands. In darkness, active ion channels in the plasma membranes of photoreceptors drive ATP consumption by stimulating the activity ion pumps needed to maintain normal ion gradients. In light, metabolic energy is used to fuel phototransduction and to support synthesis of lipid and proteins (Ames, Li, Heher, & Kimble, 1992; Cornwall et al., 2003; Okawa, Sampath, Laughlin, & Fain, 2008).

Energy metabolism in the vertebrate retina is dominated by aerobic glycolysis, also called the Warburg effect. Between 80% and 96% of glucose consumed by an isolated retina is made into lactate even when O₂ is abundant (Ames et al., 1992; Du, Cleghorn, Contreras, Linton, et al., 2013; Wang, Kondo, & Bill, 1997; Winkler, 1981). Glucose is essential for retinal function. Removal of glucose, inhibition of glycolysis, or deprivation of oxygen rapidly diminishes the ability of the retina to respond to light (Ames et al., 1992; Kang Derwent & Linsenmeier, 2000). Deficiencies of key enzymes and transporters in glucose metabolism cause retinal degeneration (Bui, Kalloniatis, & Vingrys, 2004; Maurer, Schonhaler, Mueller, & Neuhaus, 2010; Ochrietor & Linser, 2004). Neurons in the retina require metabolic support from glial cells. Either disruption of Müller cell metabolism or genetic ablation of Müller cells can cause retinal degeneration (Jablonski & Iannaccone, 2000; Shen, Zhu, Lee, Chung, & Gillies, 2013). An important reason to investigate retinal metabolism is that its disruption is likely to be the basis for many forms of neurodegenerative diseases.

Metabolic analysis using stable isotopes is a powerful tool for probing enzyme reactions and transporter/carrier activities in an intact retina. Metabolites that differ in the number of isotopic atoms incorporated are called mass isotopomers. The distributions of mass isotopomers provide insights into the types of pathways in a tissue and how they are regulated. The distributions of isotopomers can be quantified by gas chromatography (GC) and/or liquid chromatography (LC) followed by mass spectrometry (MS).

We have used stable isotope methods to identify novel metabolic pathways in intact mouse retinas (Du, Cleghorn, Contreras, Lindsay, et al., 2013; Du, Cleghorn, Contreras, Linton, et al., 2013; Lindsay et al., 2014). We present our methods in detail including experiment design, retinal culture, sample preparation, mass spectrometry analysis, and examples of applications.



2. METHODS

A flow chart of the stable isotope metabolic analysis in retinas is shown in Fig. 2.

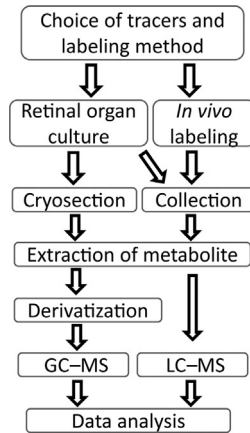


Figure 2 A flow chart of the steps in stable isotope experiments in retina.

2.1 Choice of Stable Isotope Tracers and Labeling Method

^{13}C , ^2H , ^{15}N , and ^{18}O are stable isotopes commonly used to study metabolism. Many tracers labeled with these stable isotopes at various positions are commercially available. Specific tracers can be chosen based on the types of biochemical reactions being studied. There are many reports on how to select tracers rationally for mass spectrometry. Here, we present a short list of tracers we used in retina or that will be potentially useful for future studies of retinal metabolism in [Table 1](#). Some neuronal cell types might prefer certain types of tracers, e.g., ^{13}C acetate and ^{13}C glutamate are highly preferred by astrocytes in brain metabolism ([Deelchand, Shestov, Koski, Ugurbil, & Henry, 2009](#); [Pellerin & Magistretti, 1994](#)). The types of tracers should be chosen to most effectively investigate the specific cell type and incubation conditions.

There are at least three methods to label metabolites based on the time of experiment: (1) Steady-state labeling, (2) Dynamic state (nonsteady state) labeling, and (3) Pulse-chase labeling. Steady-state labeling can take hours to days in mammalian culture depending on the pathways or types of cells and tissue. It is called steady state because the metabolic labeling pattern, concentration, and fluxes remain unchanged over time. Most flux analyses, calculations, and modeling assume that metabolites have reached steady state ([Gianchandani, Chavali, & Papin, 2010](#)). For retinas in *ex vivo* culture incubated with U- ^{13}C glucose, glycolytic intermediates reach steady state after about 90 min, but intermediates in the tricarboxylic acid (TCA) cycle require about 4 h to reach steady state ([Du, Cleghorn, Contreras, Linton, et al., 2013](#)).

Table 1 A Short List of Stable Isotope Tracers in the Study of Retinal Metabolism

Tracers	Metabolic Pathways
^{13}C glucose	Glycolysis, TCA cycle, fatty acids, PPP pathway
^{13}C glutamine	TCA cycle, IDH carboxylation, fatty acids
^{13}C glutamate	Astrocyte metabolism, glutamine metabolism
^{13}C lactate	Gluconeogenesis, TCA cycle
^{13}C pyruvate	Pyruvate transport, TCA cycle
^{13}C palmitate	Fatty acid oxidation, ketone body metabolism
^{13}C glycine	One carbon metabolism, purine synthesis
^{13}C acetate	Astrocyte metabolism, TCA cycle
^2H glucose	Glucose metabolism, NAD(P)H reaction
^{15}N glutamine	Transamination, nucleotide synthesis
^{13}C ^{15}N ATP	Purine degradation
$^2\text{H}_2\text{O}$	Lipogenesis, gluconeogenesis
H_2 ^{18}O	ATP hydrolysis and biosynthesis, cGMP metabolism, glycolysis, glycogenolysis

Steady-state labeling facilitates calculating metabolic flux accurately; however, it takes a long time and one needs to make sure that there is no loss of cell viability or changes in cellular phenotypes. Steady-state labeling also obscures dynamic information about metabolic pathways (Fernie, Geigenberger, & Stitt, 2005; Noh & Wiechert, 2011; Wiechert & Noh, 2013). Multiple cycling produces labeling patterns in which it is difficult to distinguish metabolites from different pathways. For example, under steady-state conditions U- ^{13}C glucose labeling, M3 malate can be produced either from the second turn of the TCA cycle or from the pyruvate carboxylase reaction. When dynamic labeling is used, i.e., labeling for only short time (1–5 min), the TCA metabolites have not started the second cycle. Under those conditions any M3 malate must be exclusively from carboxylation. Dynamic state labeling uses shorter incubation times with the tracer and can limit the labeling to specific pathways. However, in dynamic state labeling, differences in pool sizes should be considered for accurate calculation of metabolic flux. As the tracers have not reached equilibrium with unlabeled metabolic pools, pool sizes are inversely correlated to the rate of enrichment and can significantly affect flux calculation, especially, when comparing flux with different tissue

or treatment that alters pool sizes. The pool sizes can be measured simultaneously with the same or different tracers (Gastaldelli, Coggan, & Wolfe, 1999; Noh et al., 2007). Pulse–chase labeling starts with addition of a labeled metabolite for a brief interval (pulse) and then changes to incubation with the same metabolite in unlabeled form (chase). This technique can be very useful for analyzing pathways where metabolites are exchanged between different cells types in a tissue (see details in Section 3.1).

2.2 Retinal Organ Culture

Mammalian retinal organ cultures provide a very useful model for identifying and characterizing metabolic pathways. Its strength is that it gives investigators the flexibility to design protocols that focus on the roles of specific fuels, metabolites, and metabolic pathways. Its weakness is that it may not accurately reflect *in vivo* metabolism. We use a defined Krebs–Ringer/HEPES/bicarbonate (KRB) medium to culture mouse or rat retinas. The KRB medium has several advantages over enriched medium: (1) it minimizes interference caused by metabolites added with serum and supplements; (2) It can be customized by addition of specific nutrients or changes of solvent, e.g., with commercial enriched medium, it is hard to use ^{18}O water as a tracer; and (3) It is inexpensive. We found that retinas can maintain physiological functions (light response and O_2 consumption) in this medium. In KRB containing 5 mM glucose, there is no appreciable cell death within 6 h (based on propidium iodide staining). We prepare KRB medium in stock concentration and filter it through a 0.22 μM membrane (Table 2). The KRB is diluted to its final concentration with water. Nutrients or stable isotope tracers are added just before each experiment.

Table 2 The Formula of KRB Medium

Solute	Stock (mM)	Final (mM)	Sigma Cat.
NaCl	102.60	98.50	S5886
KCl	5.11	4.90	P5405
KH_2PO_4	1.25	1.20	P5655
MgSO_4	1.25	1.20	M1880
HEPES	20.84	20.00	H4034
CaCl_2	2.71	2.60	C7902
NaHCO_3	26.98	25.90	S5761

When ^{18}O water is used as a tracer, the components of the KRB are dissolved in 10% ^{18}O water. Light- or dark-adapted mice are euthanized by cervical dislocation. The eyes are enucleated and the retina is dissected out of the eye cup into cold HBSS under a dissecting microscope. For dark-adaptation experiments, the mice are dark-adapted for longer than 4 h. All operations including retina dissections are performed under infrared illumination with the investigator using night-vision goggles to see. Retinas are washed once with cold HBSS and then transferred into preincubated KRB medium containing nutrient and tracers of choice at 37 °C in a 5% CO_2 incubator. The entire operation from euthanasia to putting the culture dishes into the incubator should take less than 5 min to minimize hypoxia and photoreceptor cell death. Photoreceptors are very sensitive to hypoxia and nutrient deprivation. The block of blood supply for only 10 s could cause vision loss (Linsenmeier, 1990) and the availability of glucose is essential for the survival of photoreceptors (Chertov et al., 2011). Rat retinal isolation and culture are done in the same way as the mouse except the rat retina is cut into four pieces to increase nutrient accessibility.

2.3 Retinal Organ Culture for Cryosection

The unique laminated structure of retina (Fig. 1) allows the separation of different cell layers by cryosectioning (see Section 2.5.3). Our lab has used this technique to localize protein expression and metabolites in different cell layers (Du, Cleghorn, Contreras, Linton, et al., 2013; Lindsay et al., 2014; Linton et al., 2010). We have optimized this method for tracer experiments. Retinas should be flattened to ensure successful cryosectioning. A dissecting microscope is used to place the isolated retina in HBSS onto the grid side of a cellulose membrane disc (0.45 μm , 13 mm, gridded, EMD Millipore) with the photoreceptor side facing the cellulose. Cuts are made in the retina to relieve mechanical stress so that it can be flattened. To enhance attachment of the retina to the cellulose, the retina/cellulose disc is blotted quickly on filter paper and then returned to HBSS. We repeat this 3 \times and then incubate the retina/cellulose discs in 35 mM culture dishes containing 2 ml tracers and KRB.

2.4 Tracing Retinal Metabolism *In Vivo*

Studying retina metabolism *in vivo* has unique advantages. The retinas are in their native physiological environment and they are not stressed by euthanasia, dissection, or changes in their environment. *In vivo* stable-isotope

labeling has been used extensively in brain tissue together with NMR and mass spectrometry (Dobbins & Malloy, 2003; Kanamori, Kondrat, & Ross, 2003). However, to our knowledge there is no data available yet on stable-isotope labeling of retinas *in vivo*. Our preliminary experiments have shown that intraperitoneal injection of a bolus of U-¹³C glucose (500 mg/Kg) enriched the glycolysis and TCA cycle intermediates (listed in Table 2) between 10% and 40% in 45 min in mouse retina. In this experiment, the retina was isolated quickly from the mouse and snap frozen in liquid nitrogen (Section 2.5.2). More *in vivo* studies will be needed to optimize this method to explore labeling of retinas through intravenous and intravitreal injection and infusion, and to determine the influence of permeability of retinal-blood barrier on the choice of tracers that can be used. However, some disadvantages in *in vivo* labeling should also be considered in experiment design: (1) Multiple and bigger pools compared with *ex vivo* culture can take longer to reach isotopic steady state; (2) Metabolism and metabolic exchange among tissues (e.g., Cori cycle between muscle and liver) can result in scrambling of mass isotopomers; (3) The patterns of mass isotopomers distribution (MID) and time to reach steady state can be influenced by the sites (intraperitoneal, tail vein, or intravitreal injections) of tracer administration.

2.5 Sample Collection and Preparation

Good sample preparation is the starting point for successful metabolite analysis. Since cellular metabolites have very rapid turnover, sample collection and preparation require the fastest possible quenching and most effective extraction of cellular metabolites. There are many reports on quenching and extraction methods. We found it is effective to quench the reaction with cold saline (Strumilo, 1995) and extract polar metabolites with a cold methanol/chloroform/water mixture. To obtain spatial resolution of the metabolic reaction, the retina can be sliced into sections to separate cell layers. For GC-MS, the extract metabolites need to be derivatized to render them volatile.

2.5.1 Collection and Preparation of Medium Sample

We collect KRB medium samples directly into EP tubes and centrifuge them at 14,000 rpm for 10 min. The supernatant is transferred and saved at -20 °C. Glucose and glutamine can be analyzed by LC-MS (see Section 2.5) or by commercial colorimetric analysis such as Amplex red assays (Life Sciences). Lactate, pyruvate, citrate, adenosine, and

hypoxanthine are often released by mouse retinas, so they can be measured by GC–MS and LC–MS. We transfer 20–50 μl of medium into an insert (Agilent) inside a 1.5 EP tube and dry it for derivatization for GC–MS, or we transfer it into an EP tube and dry it for LC–MS. It is important to note that high salt concentration can suppress mass spectrometry signals. To test for this effect in LC–MS, we redissolved the dried sample in $2 \times$ volume of mobile phase and compared it to dissolving the standard directly in the mobile phase. There is no significant difference in the signals we detected in most of our samples. However, if larger volumes of sample medium are used, the salt should be removed by ion exchange columns before analysis.

2.5.2 Collection and Preparation of Retinas

After labeling *ex vivo* or *in vivo*, the retina is transferred quickly into a 1.5 ml conical screw cap tube containing 1 ml ice cold 0.9% NaCl to quench metabolism. We often use a transfer pipette or wide-opening 1 ml pipette tip to transfer the retina to avoid damage. The tube is spun quickly to remove cold saline and immediately frozen in liquid nitrogen. In advance, we prepare extraction buffer (methanol:chloroform:H₂O (700:200:50)) and store it on ice. We add 140 μl of this extraction buffer together with 10 μl of 100 μM methylsuccinate or norvaline into the tube. These are added as internal standards. We homogenize the retina with pestles powered by a cordless motor (Kimble-Kontes) for 15 s and leave the homogenate on ice for 15 min to precipitate proteins. The homogenate then is centrifuged at 14,000 rpm for 15 min at 4 °C and the supernatant containing extracted metabolites is transferred to a 250 μl glass insert placed inside a 1.5 ml EP tube. The sample can be dried for mass spectrometry or stored at –80 °C. The pellet is dissolved in 200 μl of 0.1 M NaOH overnight at 37 °C. Protein concentrations are determined by the BCA assay kit (Thermo Fisher Scientific). *Note: Be careful when taking the tube out of centrifuge to avoid loosening the pellet.*

2.5.3 Cryosection of Labeled Retina

The retina/cellulose disc (from [Section 2.3](#)) is picked up with forceps, being careful not to touch the retina. The disc is dipped into a dish containing cold 0.9% NaCl for 5 s to quench metabolism. We place the disc with its cellulose side down (the side without the retina) on filter paper to dry the liquid quickly. We mount the disc with the same side down, on a quarter of a glass slide prepared with a small drop of superglue on its top. The slide is then snap frozen under slight pressure on a drill

press. In preparation for this, the head of a bolt that has been polished to a mirror finish is kept cold in liquid nitrogen. Just before flattening the retina we insert the bolt into the chuck of a drill press and tighten it in place. The head of the bolt is lowered quickly onto the retina and contact is made with slight pressure for ~ 5 s. After freezing, the retina/cellulose slide is stored on dry ice.

A second quarter of a glass slide then is wrapped in polytetrafluoroethylene (PTFE) tape. This is to prevent the retina from sticking to the slide. A ~ 0.5 mm plastic spacer is glued on each side of the PTFE tape. Then we sandwich the retina/cellulose between the slides. Binder clips are used to hold the sandwich together. The sandwiched retina then is placed on dry ice for 30 min and stored overnight at -20 °C.

We then cover a cryostat pedestal in optimal cutting temperature compound (OCT) and allow it to freeze completely. The OCT covered pedestal is mounted in the cryostat and 20 μm slices are made until the OCT is completely flat in one plane. We disassemble the retina sandwich and mount the retina/cellulose slide on the flat OCT pedestal. We use a drop of water applied to the top corners of the slide OCT interface and allow it to freeze in place.

We trim the flattest part of the retina with a scalpel blade to an area ~ 1 mm^2 . After trimming, the cryostat blade is advanced in 20 μm steps until contact has been made with the trimmed retina. Sections are then cut at 50 μm until contact with the cellulose. At this thickness, the outer segment layer, photoreceptor cell body layer, inner retina layer, and ganglion cell layer are included in a total of 4–5 sections (Fig. 1). Each section is picked up with a plastic pipette tip and placed into a 1.5 ml tube containing extraction buffer on dry ice. The metabolites are extracted as described in Section 2.5.2. The pellet is dissolved in protein lysis buffer. The quality of the sectioning is monitored by immunoblotting with antibodies against photoreceptor or ganglion cell specific markers.

2.5.4 Derivatization for GC–MS

GC–MS requires all analytes to be volatilized. The polar nature of amino acids and organic acids requires derivatization before GC analysis. Depending on the metabolites of interest, there are a large variety of derivatization reagents and methods available for GC–MS. Here, we provide a protocol to derivatize keto groups with methoxyamine and to replace hydrogen groups in COOH, NH, and SH with volatile *N*-tert-butyltrimethylsilyl-*N*-methyltrifluoroacetamide (TBDMS). The derivatives

from this method are more stable and less moisture sensitive than most other types of derivatives. We use the following protocol:

1. Dry the samples (as prepared in [Sections 2.5.1–2.5.3](#)) in a lyophilizer (Labconco) or Speedvac without heat until they are completely dry.
2. Add 25 μl of freshly prepared methoxyamine hydrochloride (Sigma) in pyrimidine (20 mg/ml) to the dried whole retinal extract. For dried retinal sections or dried medium samples use only 10 μl . Gently tap the tubes with inserts inside 3–5 \times to mix, then spin the samples down and close the lid tightly.
3. Incubate them at 37 $^{\circ}\text{C}$ for 90 min in an oven or heat block.
4. After incubation, quickly spin the tubes and transfer into the inserts, 25 μl for whole retinal extract, 10 μl for section extract or 10 μl for medium sample. Gently tap the tubes 3–5 \times to mix, then spin the samples and close the lid tightly.
5. Incubate the tubes with samples inside at 70 $^{\circ}\text{C}$ for 30 min. Spin tubes and transfer inserts into GC–MS glass vials. For medium samples, the supernatant will be transferred to new inserts in glass vials. The sample should be clear after derivatization although they may be colored from drugs used in the incubations. If it is yellowish, the sample might be contaminated with proteins during preparation.

2.5.5 Sample Preparation for LC–MS

Samples to be analyzed by LC–MS do not need derivatization. The retinal samples are dried completely and suspended in 100 μl of mobile phase (40% of A and 60% of B) with vortex for 10 s. The samples are then passed through 0.45- μM PVDF syringe filters directly into glass inserts in vials.

2.6 Analysis of Metabolites by GC–MS

GC–MS is used to measure metabolites including most of the intermediates in glycolysis and the TCA cycle ([Table 3](#)). We use an Agilent 7890/5975C GC/MS system (Agilent Technologies) with an Agilent HP-5MS column (30 m \times 0.25 mm \times 0.25 μm film) under electron ionization at 70 eV. Ultrahigh-purity helium is the carrier gas at a constant flow rate of 1 ml/min. One microliter of sample is injected in split-less mode by the auto sampler. The temperature gradient starts at 100 $^{\circ}\text{C}$ with a hold time of 4 min and then increases at a rate of 5 $^{\circ}\text{C}/\text{min}$ to 300 $^{\circ}\text{C}$, where it is held for 5 min. The temperatures reset as follows: inlet 250 $^{\circ}\text{C}$, transfer line 280 $^{\circ}\text{C}$, ion source 230 $^{\circ}\text{C}$, and quadrupole 150 $^{\circ}\text{C}$. Mass spectra are collected from m/z 50–600 at a rate of 1.4 spectra/s after a 6.5-min solvent delay. Select ion

Table 3 Metabolites for GC–MS Analysis

Metabolite	M-57 Ion	OH/NH/SH + Keto	Metabolite Formula	Derivative Formula	SIM	RT (Min)
Metabolites in glycolysis						
3PG	585	4	C ₃ H ₃ O ₇ P	Si ₄ C ₂₀ H ₅₁	585–588	35.81
GAP	484	3 + 1	C ₃ H ₄ O ₆ P	Si ₃ C ₁₅ H ₃₉ N	484–487	31.71
DHAP	484	3 + 1	C ₃ H ₄ O ₆ P	Si ₃ C ₁₅ H ₃₉ N	484–487	32.08
PEP	453	3	C ₃ H ₂ O ₆ P	Si ₃ C ₁₄ H ₃₆	453–456	29.50
Pyruvate	174	1 + 1	C ₃ H ₃ O ₃	SiC ₃ H ₉ N	174–177	8.50
Lactate	261	2	C ₃ H ₄ O ₃	Si ₂ C ₈ H ₂₁	261–264	14.39
Alanine	260	2	C ₃ H ₅ NO ₂	Si ₂ C ₈ H ₂₁	260–263	15.51
Serine	390	3	C ₃ H ₄ NO ₃	Si ₃ C ₁₄ H ₃₆	390–393	25.12
Metabolites in TCA cycle						
Citrate	591	4	C ₆ H ₄ O ₇	Si ₄ C ₂₀ H ₅₁	591–597	35.66
α-Ketoglutarate	346	2 + 1	C ₅ H ₄ O ₅	Si ₂ C ₉ H ₂₄ N	346–351	25.57
Malate	419	3	C ₄ H ₃ O ₅	Si ₃ C ₁₄ H ₃₆	419–423	27.40
Succinate	289	2	C ₄ H ₄ O ₄	Si ₂ C ₈ H ₂₁	289–293	20.52
Fumarate	287	2	C ₄ H ₂ O ₄	Si ₂ C ₈ H ₂₁	287–291	21.14
Aspartate	418	3	C ₄ H ₄ NO ₄	Si ₃ C ₁₄ H ₃₆	418–422	28.19
Glutamate	432	3	C ₅ H ₆ NO ₄	Si ₃ C ₁₄ H ₃₆	432–437	30.26
Glutamine	431	3	C ₅ H ₇ N ₂ O ₃	Si ₃ C ₁₄ H ₃₆	431–436	32.67
Asparagine	417	3	C ₄ H ₅ N ₂ O ₃	Si ₃ C ₁₄ H ₃₆	417–421	30.73
2-HG	433	3	C ₅ H ₅ O ₅	Si ₃ C ₁₄ H ₃₆	433–438	29.22
NAA	460	3	C ₆ H ₆ NO ₅	Si ₃ C ₁₄ H ₃₆	460–466	30.93
3HBA	275	2 + 1	C ₄ H ₆ O ₃	Si ₂ C ₉ H ₂₄ N	275–279	16.93
IS						
Methylsuccinate	303	2	C ₅ O ₄ H ₆	Si ₂ C ₈ H ₂₁	303	20.70
Norvaline	288	2	C ₅ H ₉ NO ₂	Si ₂ C ₈ H ₂₁	288	18.42

3PG, 3-phosphoglycerate; GAP, glyceraldehyde 3-phosphate; DHAP, dihydroxyacetone phosphate; PEP, phosphoenolpyruvic acid; IS, internal standard.

monitoring (SIM) records only selected ranges of m/z in expected retention time windows. This mode significantly improves the sensitivity and specificity of detection.

The TBDMS group adds 114 and methoxyamine adds 29 to the molecular weight. After ionization, the molecular weight 57 less than the derivatives (C₄H₉ (M-57)) is often the major ion in the spectra. Therefore, M-57 mass is selected to quantify the intensity of each metabolite. Table 3 lists the mass we monitor in the SIM mode for metabolites from glucose, glutamine, and ketone metabolism. The chromatograms are analyzed using Agilent Chemstation software. Abundances of the selected ions are extracted.

Natural abundance from stable isotopes and derivative agents interferes with the MID, and it must be corrected before MID analysis (Fernandez, Des Rosiers, Previs, David, & Brunengraber, 1996; Hellerstein & Neese, 1999). IsoCor, freely available software under an open-source license, provides a simple solution to correct both common naturally occurring isotopes (C, H, O, S, N, and Si) and the purity of the isotopic tracer (Millard, Letisse, Sokol, & Portais, 2012) (<http://metasys.insa-toulouse.fr/software/isocor>). The metabolite formula (the formula after derivatization) and derivative formula listed in Table 3 can be used in IsoCor for natural abundance correction. The fractional abundance of isotopomers are named as M₀, M₁, M₂, ..., M_x. M₀ is the mass without labeling (M-57 ion in Table 3) and 1 to x represents the mass shift from the isotope labeling.

The concentration of each unlabeled metabolite is determined using an external calibration curve containing internal standard.

2.7 Analysis of Metabolites by LC-MS

Large and/or thermo-unstable organic molecules including sugars, phosphate, and nucleotides are particularly suitable for LC-MS. There are a large selection of methods and instruments available depending on the metabolites of interest. Labeled glucose, glutamine, and glutathione from ¹³C glucose or ¹³C glutamine in the medium and retina can be quantified directly by LC-MS. Analysis of the mass isotopomer distributions of nucleotides can estimate the rate of ATP production, cGMP degradation, and pathways in nucleotide degradation. Here, we present a protocol to measure metabolites listed in Table 4 by LC-MS. We use a Waters Xevo TQ Tandem mass spectrometer with a Waters ACQUITY system with UPLC. An ACQUITY UPLC BEH Amide analytic column (2.1 × 50 mm, 1.7 μm, Waters) is used for separation. The mobile phase is (A) water with

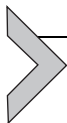
Table 4 Metabolites for LC–MS Analysis

Metabolite	Mode	Parent (<i>m/z</i>)	Daughter (<i>m/z</i>)	Dwell (s)	Cone (v)	Collision (v)
Glucose	Negative	179	89	0.025	18	8
Glutamine	Positive	147	84	0.025	14	16
GSSH	Positive	613	231	0.04	86	38
GSH	Positive	308	84	0.04	22	22
ATP	Positive	508	136	0.08	28	30
ADP	Negative	426	134	0.025	34	22
AMP	Negative	346	79	0.025	34	22
Adenosine	Positive	268	136	0.06	22	16
NAD	Positive	664	136	0.025	28	52
NADH	Positive	666	108	0.06	24	58
GTP	Negative	521	159	0.04	40	34
cGMP	Positive	346	135	0.06	30	44
GDP	Positive	444	135	0.06	20	60
GMP	Positive	364	135	0.06	20	46
Guanosine	Positive	284	152	0.06	14	16
Xanthine	Negative	151	108	0.025	32	14
Hypoxanthine	Negative	135	92	0.025	32	14

GSH, reduced glutathione; GSSH, oxidized glutathione; cGMP, cyclic GMP.

10 mM ammonium acetate (pH 8.9) and (B) acetonitrile/water (95/5) with 10 mM ammonium acetate (pH 8.9) (All solvents are LC–MS Optima grade from Fisher Scientific). The gradient elution is (1) 95–61% B in 6 min, (2) 61–44% B at 8 min, (3) 61–27% B at 8.2 min, and 27–95% B at 9 min. The column is reequilibrated with 95% B at the end of each run. The Flow rate for all gradient is 0.5 ml/min and the total run is 11 min. The injection volume for each sample is 5 μ l. Mass spectrometer settings are shown in Table 4. Each transition includes a parent ion and fragmented daughter ion. Transitions for isotopomers can be set up based on the tracers. *A priori* knowledge of the labeled moiety on the parent and/or daughter ions is important. The formula and fragment pattern can be checked in public databases such as METLIN (<http://metlin.scripps.edu/index.php>) and Human Metabolome

Database (<http://www.hmdb.ca/>). For example, the daughter ion of ATP is the purine base. In ^{18}O water tracer experiments, the transitions of isotopomers of parent ions can be set at 508 (M0), 510 (M2), 512 (M4), and 514 (M6), while the daughter ion is 136 for all these transitions since purine base will not be labeled by ^{18}O . The chromatograms are analyzed by MassLynx (Waters). Corrections for natural abundance are made as described in the section on GC–MS.



3. APPLICATIONS

3.1 Neuron–Glia Interaction

Müller glia interact closely with neurons to maintain metabolic homeostasis. Müller cells quickly undergo reactive gliosis after neuronal damage and similarly the damage of Müller cells can cause the death of photoreceptor neurons (Dyer & Cepko, 2000; Shen et al., 2013). This interdependence might be attributed to the intricate metabolite exchange between glia and neurons. It has been hypothesized that Müller glia supply glutamine and glucose to neurons while neurons might send lactate and glutamate to Müller glial cells. Stable-isotope labeling has been proved to be a useful tool to understand the metabolic interactions between glia and neurons in retina (Lindsay et al., 2014).

An example from our lab demonstrates that glia can use lactate and aspartate from neurons as surrogates to compensate for specific enzyme deficiencies in the Müller cells (Lindsay et al., 2014). We found that photoreceptors have abundant expression of both pyruvate kinase M2 isoform (PKM2) and aspartate glutamate carrier 1 (AGC1), but there is very little expression of these two enzymes or any other forms of pyruvate kinase in Müller glial cells. Glutamine synthetase (GS) is expressed exclusively in Müller glia in retinas, where it produces glutamine for neurons. To understand how Müller glia overcome their deficiency in Pyruvate Kinase and AGC1 in glutamine synthesis, we labeled retinas and isolated cells with different ^{13}C labeled fuels, and found that ^{13}C aspartate is the most efficient fuel for glial cells. Aspartate enhanced glycolysis, the TCA cycle, and glutamine synthesis in both intact retina and isolated glial cells. To test our hypothesis that aspartate transports oxidizing power and carbons from neurons to Müller cells in intact retinas, we designed a pulse-chase labeling strategy. This strategy is based on our results and *a priori* knowledge about glutamine/glutamate metabolism. The photoreceptors are the primary site of glutamine catabolism and Müller cells are the primary site of glutamine synthesis. Glutaminase mostly

expresses in neurons and GS is exclusively in MCs. To test the strategy, we treated retinas for 5 min with 5 mM U- ^{13}C glutamine (M5), followed by incubation with 5 mM unlabeled lactate. Unlabeled glutamine was not included in the chase, because the intense signal from the added glutamine would have obscured the isotopomer signals we intended to quantify. At various times, retinas were harvested and metabolites were extracted and analyzed by GC-MS as described in Section 2. Figure 3A tracks the flow of carbons in this model. Figure 3B (upper) shows that M5 Glutamine

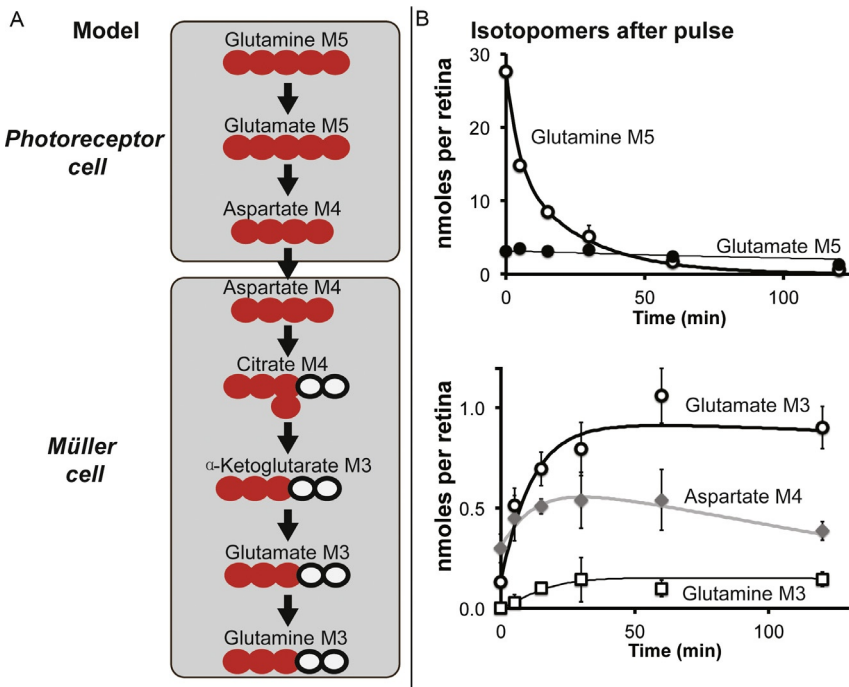


Figure 3 Pulse-chase analysis of U- ^{13}C Gln in retina. Data are taken from the authors' previous study (Lindsay et al., 2014). (A) Schematic model for the role of aspartate as a carrier of oxidizing power between retinal neurons and glia. Red circles represent the ^{13}C carbons, and black circles represent the ^{12}C carbons. (B) ^{13}C labeling of Aspartate, Glutamate, and Glutamine from the pulse of U- ^{13}C Glutamine. (Upper) The M5 Glutamine and Glutamate are derived directly from the pulse of 5 mM U- ^{13}C Glutamine. After 5 min, the medium was changed to 5 mM unlabeled Lac with no added Gln. The retinas were subsequently harvested at the indicated times after the pulse. (Lower) The M4 Aspartate derived from oxidation of Glutamate via the TCA. The M3 Glutamate is made by further oxidation via citrate, and M3 Glutamine is made only in MCs by Glutamine synthetase ($n = 6$).

converts rapidly to M5 Glutamate. The lingering M5 glutamate and M5 α -ketoglutarate are consistent with our previously reported finding that α -ketoglutarate in retinas is protected from oxidation in neurons. [Figure 3B](#) (lower) shows how M4 aspartate accumulates and then decays as M3 Glutamate and then M3 Glutamine accumulate. Conversion of M4 aspartate into M3 Glutamine confirms that the subsequent reactions ([Fig. 3A](#)) occur in MCs, because only MCs express GS. We further confirmed this model by blocking the transport of aspartate. The availability of more information on differential enzyme distribution, animal models of specific cell ablation, and models of conditional gene knockout will substantially facilitate further advance in understanding of metabolic interactions using stable isotope-based methodologies.

3.2 Retinal Metabolism in Light and Dark Adaption

Many studies have shown that both energy demand and energy production in retinas are greater in darkness than in light ([Ames et al., 1992](#); [Cornwall et al., 2003](#); [Linsenmeier, 1986](#); [Okawa et al., 2008](#); [Wang et al., 1997](#)). Photoreceptors are constitutively depolarized in darkness because ion channels in the outer segment of the photoreceptor are opened by their agonist, cyclic GMP. Ions leaking in through those channels in darkness must be removed from the cell via an ion pump that consumes ATP. Light activates cGMP hydrolysis to close channels and diminish ATP consumption but light also stimulates specific anabolic requirements, regeneration of visual pigment, and renewal of membranes. The molecular mechanisms by which retinas control the pace of their metabolism under different illumination conditions are still unknown. Energy consumption in retina has been evaluated by measuring O_2 consumption, production of CO_2 and lactate, and pumping of sodium ion ([Okawa et al., 2008](#); [Wang et al., 1997](#); [Winkler, 1981](#)). These experiments have limitations in providing mechanistically biochemical insights. Furthermore, besides energy consumption, little information is available on changes of nucleotide metabolism in light and darkness. This is important because large changes in cGMP metabolism could alter metabolism of other purines as well. Stable isotope tracers can be used with light- and dark-adapted retinas both *ex vivo* and *in vivo*. These tracers can monitor metabolic enzyme reactions directly by measuring the labeled metabolites. Cryosection of labeled retinal layers will provide information about the metabolic changes occurring in the retina.

3.3 Retinal Degenerative Diseases

Retinal degenerative diseases cause blindness in both young and old in a variety of diseases including age-related macular degeneration (AMD), retinitis pigmentosa, Leber's congenital amaurosis, Stargardt disease, and Usher Syndrome (Rejda et al., 2012). Retinal degenerative diseases have been linked to mutations in energy metabolism and purine metabolism such as isocitrate dehydrogenase 3b, pyruvate dehydrogenase E1/2, nicotinamide mononucleotide adenylyltransferase, inosine monophosphate dehydrogenase, phosphodiesterase 6, and guanylyl cyclase (Aherne et al., 2004; Dizhoor, Boikov, & Olshevskaya, 1998; Farber & Lolley, 1974; Hartong et al., 2008; Maurer et al., 2010; Perrault et al., 2012; Taylor, Hurley, Van Epps, & Brockerhoff, 2004). Disruption of nutrient availability and metabolic regulation might play important roles in AMD and several models of retinitis pigmentosa (Punzo, Kornacker, & Cepko, 2009; Umino et al., 2006). The diseased neurons might reprogram metabolism and/or cause some sort of metabolic failure during degeneration. The stable isotope-based methodologies allow for kinetic analysis of metabolic reactions in diseased retinas that will help advance our understanding of these diseases. Because metabolites are very sensitive to environmental changes and cellular metabolic state, it is important to compare mutant animals with littermate controls with the same age. It also is important to include several time points spanning the full time course of the degeneration. Besides research in *ex vivo* labeling, the labeling of retinas *in vivo* will be critical to provide information on the integrity of the blood-retinal barriers and the efficiency of nutrient utilization.



4. SUMMARY

Retina is an excellent model for studying metabolism that occurs within a nonhomogeneous, multicellular tissue. Its laminar structure is suited for cryosection analysis with or without culture. Recent advances in metabolite imaging directly on tissue sections with mass spectrometry such as MALDI (matrix assisted laser desorption and ionization)-MS (Sun et al., 2014), SIMS (second ion mass spectrometry) (Wedlock et al., 2011), and NIMS (nanostructure-initiator mass spectrometry) (Greving, Patti, & Siuzdak, 2011) would help resolve the conundrum of metabolite compartmentalization and exchange among different cells in the normal and diseased retinas. Vertebrate retinas share some features of tumor

metabolism, such as Warburg effect and high expression of PKM2. They also have their own unique metabolic demands and pathways in light and darkness and in neurons and glial cells. Stable isotope-assisted methods have been successfully applied in metabolism research including retinal metabolism. The findings in cancer metabolism are useful to guide studies of retinal metabolism. Similarly, the heterogeneous nature of metabolism in retina with its different cell types might provide useful examples for tumor metabolism research. In this chapter, we have described methods we use to probe metabolism in intact retinas using stable isotopes. We first discussed how to design experiments, to choose tracers and labeling methods. We then detailed our protocols for use of retinal organ culture, cryosectioning of retinas, sample preparation, and analysis of samples by both GC-MS and LC-MS. Finally, we gave examples of our research and discussed the application of the methods to several areas of retinal metabolism research including neuron-glia interaction, light and dark adaptation, and degenerative diseases.

ACKNOWLEDGMENTS

Research on retinal metabolism in Hurley lab is funded by National Eye Institute Grants (EY06641 and EY023346). J.D. is supported by the Career Starter Award from the Knights Templar Eye Foundation.

REFERENCES

- Aherne, A., Kennan, A., Kenna, P. F., McNally, N., Lloyd, D. G., Alberts, I. L., et al. (2004). On the molecular pathology of neurodegeneration in IMPDH1-based retinitis pigmentosa. *Human Molecular Genetics*, *13*(6), 641–650.
- Ames, A., 3rd, Li, Y. Y., Heher, E. C., & Kimble, C. R. (1992). Energy metabolism of rabbit retina as related to function: High cost of Na⁺ transport. *The Journal of Neuroscience*, *12*(3), 840–853.
- Bui, B. V., Kalloniatis, M., & Vingrys, A. J. (2004). Retinal function loss after monocarboxylate transport inhibition. *Investigative Ophthalmology & Visual Science*, *45*(2), 584–593.
- Campbell, M., & Humphries, P. (2012). The blood-retina barrier: Tight junctions and barrier modulation. *Advances in Experimental Medicine and Biology*, *763*, 70–84.
- Chertov, A. O., Holzhausen, L., Kuok, I. T., Couron, D., Parker, E., Linton, J. D., et al. (2011). Roles of glucose in photoreceptor survival. *The Journal of Biological Chemistry*, *286*(40), 34700–34711.
- Cornwall, M. C., Tsina, E., Crouch, R. K., Wiggert, B., Chen, C., & Koutalos, Y. (2003). Regulation of the visual cycle: Retinol dehydrogenase and retinol fluorescence measurements in vertebrate retina. *Advances in Experimental Medicine and Biology*, *533*, 353–360.
- Cunha-Vaz, J., Bernardes, R., & Lobo, C. (2011). Blood-retinal barrier. *European Journal of Ophthalmology*, *21*(Suppl. 6), S3–S9.
- Deelchand, D. K., Shestov, A. A., Koski, D. M., Ugurbil, K., & Henry, P. G. (2009). Acetate transport and utilization in the rat brain. *Journal of Neurochemistry*, *109*(Suppl. 1), 46–54.

- Dizhoor, A. M., Boikov, S. G., & Olshevskaya, E. V. (1998). Constitutive activation of photoreceptor guanylate cyclase by Y99C mutant of GCAP-1. Possible role in causing human autosomal dominant cone degeneration. *The Journal of Biological Chemistry*, 273(28), 17311–17314.
- Dobbins, R. L., & Malloy, C. R. (2003). Measuring in-vivo metabolism using nuclear magnetic resonance. *Current Opinion in Clinical Nutrition and Metabolic Care*, 6(5), 501–509.
- Dowling, J. E. (1970). Organization of vertebrate retinas. *Investigative Ophthalmology*, 9(9), 655–680.
- Du, J., Cleghorn, W. M., Contreras, L., Lindsay, K., Rountree, A. M., Chertov, A. O., et al. (2013). Inhibition of mitochondrial pyruvate transport by zaprinstat causes massive accumulation of aspartate at the expense of glutamate in the retina. *The Journal of Biological Chemistry*, 288(50), 36129–36140.
- Du, J., Cleghorn, W., Contreras, L., Linton, J. D., Chan, G. C., Chertov, A. O., et al. (2013). Cytosolic reducing power preserves glutamate in retina. *Proceedings of the National Academy of Sciences of the United States of America*, 110(46), 18501–18506.
- Dyer, M. A., & Cepko, C. L. (2000). Control of Muller glial cell proliferation and activation following retinal injury. *Nature Neuroscience*, 3(9), 873–880.
- Farber, D. B., & Lolley, R. N. (1974). Cyclic guanosine monophosphate: Elevation in degenerating photoreceptor cells of the C3H mouse retina. *Science*, 186(4162), 449–451.
- Fernandez, C. A., Des Rosiers, C., Previs, S. F., David, F., & Brunengraber, H. (1996). Correction of ¹³C mass isotopomer distributions for natural stable isotope abundance. *Journal of Mass Spectrometry*, 31(3), 255–262.
- Fernie, A. R., Geigenberger, P., & Stitt, M. (2005). Flux an important, but neglected, component of functional genomics. *Current Opinion in Plant Biology*, 8(2), 174–182.
- Gastaldelli, A., Coggan, A. R., & Wolfe, R. R. (1999). Assessment of methods for improving tracer estimation of non-steady-state rate of appearance. *Journal of Applied Physiology*, 87(5), 1813–1822.
- Gianchandani, E. P., Chavali, A. K., & Papin, J. A. (2010). The application of flux balance analysis in systems biology. *Wiley Interdisciplinary Reviews. Systems Biology and Medicine*, 2(3), 372–382.
- Greving, M. P., Patti, G. J., & Siuzdak, G. (2011). Nanostructure-initiator mass spectrometry metabolite analysis and imaging. *Analytical Chemistry*, 83(1), 2–7.
- Hartong, D. T., Dange, M., McGee, T. L., Berson, E. L., Dryja, T. P., & Colman, R. F. (2008). Insights from retinitis pigmentosa into the roles of isocitrate dehydrogenases in the Krebs cycle. *Nature Genetics*, 40(10), 1230–1234.
- Hellerstein, M. K., & Neese, R. A. (1999). Mass isotopomer distribution analysis at eight years: Theoretical, analytic, and experimental considerations. *The American Journal of Physiology*, 276(6 Pt. 1), E1146–E1170.
- Jablonski, M. M., & Iannaccone, A. (2000). Targeted disruption of Muller cell metabolism induces photoreceptor dysmorphogenesis. *Glia*, 32(2), 192–204.
- Kanamori, K., Kondrat, R. W., & Ross, B. D. (2003). ¹³C enrichment of extracellular neurotransmitter glutamate in rat brain—Combined mass spectrometry and NMR studies of neurotransmitter turnover and uptake into glia in vivo. *Cellular and Molecular Biology (Noisy-le-Grand, France)*, 49(5), 819–836.
- Kang Derwent, J., & Linsenmeier, R. A. (2000). Effects of hypoxemia on the a- and b-waves of the electroretinogram in the cat retina. *Investigative Ophthalmology & Visual Science*, 41(11), 3634–3642.
- Lindsay, K. J., Du, J., Sloat, S. R., Contreras, L., Linton, J. D., Turner, S. J., et al. (2014). Pyruvate kinase and aspartate-glutamate carrier distributions reveal key metabolic links between neurons and glia in retina. *Proceedings of the National Academy of Sciences of the United States of America*, 111(43), 15579–15584.

- Linsenmeier, R. A. (1986). Effects of light and darkness on oxygen distribution and consumption in the cat retina. *The Journal of General Physiology*, 88(4), 521–542.
- Linsenmeier, R. A. (1990). Electrophysiological consequences of retinal hypoxia. *Graefe's Archive for Clinical and Experimental Ophthalmology*, 228(2), 143–150.
- Linton, J. D., Holzhausen, L. C., Babai, N., Song, H., Miyagishima, K. J., Stearns, G. W., et al. (2010). Flow of energy in the outer retina in darkness and in light. *Proceedings of the National Academy of Sciences of the United States of America*, 107(19), 8599–8604.
- Maurer, C. M., Schonthaler, H. B., Mueller, K. P., & Neuhauss, S. C. (2010). Distinct retinal deficits in a zebrafish pyruvate dehydrogenase-deficient mutant. *The Journal of Neuroscience*, 30(36), 11962–11972.
- Millard, P., Letisse, F., Sokol, S., & Portais, J. C. (2012). IsoCor: Correcting MS data in isotope labeling experiments. *Bioinformatics*, 28(9), 1294–1296.
- Newman, E., & Reichenbach, A. (1996). The Muller cell: A functional element of the retina. *Trends in Neurosciences*, 19(8), 307–312.
- Noh, K., Gronke, K., Luo, B., Takors, R., Oldiges, M., & Wiechert, W. (2007). Metabolic flux analysis at ultra short time scale: Isotopically non-stationary ¹³C labeling experiments. *Journal of Biotechnology*, 129(2), 249–267.
- Noh, K., & Wiechert, W. (2011). The benefits of being transient: Isotope-based metabolic flux analysis at the short time scale. *Applied Microbiology and Biotechnology*, 91(5), 1247–1265.
- Ochrietor, J. D., & Linsler, P. J. (2004). 5A11/Basigin gene products are necessary for proper maturation and function of the retina. *Developmental Neuroscience*, 26(5–6), 380–387.
- Okawa, H., Sampath, A. P., Laughlin, S. B., & Fain, G. L. (2008). ATP consumption by mammalian rod photoreceptors in darkness and in light. *Current Biology*, 18(24), 1917–1921.
- Pellerin, L., & Magistretti, P. J. (1994). Glutamate uptake into astrocytes stimulates aerobic glycolysis: A mechanism coupling neuronal activity to glucose utilization. *Proceedings of the National Academy of Sciences of the United States of America*, 91(22), 10625–10629.
- Perrault, I., Hanein, S., Zanlonghi, X., Serre, V., Nicouleau, M., Defoort-Delhemmes, S., et al. (2012). Mutations in NMNAT1 cause Leber congenital amaurosis with early-onset severe macular and optic atrophy. *Nature Genetics*, 44(9), 975–977.
- Punzo, C., Kornacker, K., & Cepko, C. L. (2009). Stimulation of the insulin/mTOR pathway delays cone death in a mouse model of retinitis pigmentosa. *Nature Neuroscience*, 12(1), 44–52.
- Rejdak, R., Szkaradek, M., Czepita, M., Taslaq, W., Lewicka-Chomont, A., & Grieb, P. (2012). Retinal degenerative diseases—Mechanisms and perspectives of treatment. *Klinika Oczna*, 114(4), 301–307.
- Shen, W., Zhu, L., Lee, S. R., Chung, S. H., & Gillies, M. C. (2013). Involvement of NT3 and P75(NTR) in photoreceptor degeneration following selective Muller cell ablation. *Journal of Neuroinflammation*, 10, 137.
- Strumilo, E. (1995). Effect of Ca²⁺ on the activity of mitochondrial NADP-specific isocitrate dehydrogenase from rabbit adrenals. *Acta Biochimica Polonica*, 42(3), 325–328.
- Sun, N., Ly, A., Meding, S., Witting, M., Hauck, S. M., Ueffing, M., et al. (2014). High-resolution metabolite imaging of light and dark treated retina using MALDI-FTICR mass spectrometry. *Proteomics*, 14(7–8), 913–923.
- Taylor, M. R., Hurley, J. B., Van Epps, H. A., & Brockerhoff, S. E. (2004). A zebrafish model for pyruvate dehydrogenase deficiency: Rescue of neurological dysfunction and embryonic lethality using a ketogenic diet. *Proceedings of the National Academy of Sciences of the United States of America*, 101(13), 4584–4589.

- Umino, Y., Everhart, D., Solessio, E., Cusato, K., Pan, J. C., Nguyen, T. H., et al. (2006). Hypoglycemia leads to age-related loss of vision. *Proceedings of the National Academy of Sciences of the United States of America*, 103(51), 19541–19545.
- Wang, L., Kondo, M., & Bill, A. (1997). Glucose metabolism in cat outer retina. Effects of light and hyperoxia. *Investigative Ophthalmology & Visual Science*, 38(1), 48–55.
- Wassle, H., & Boycott, B. B. (1991). Functional architecture of the mammalian retina. *Physiological Reviews*, 71(2), 447–480.
- Wedlock, L. E., Kilburn, M. R., Cliff, J. B., Filgueira, L., Saunders, M., & Berners-Price, S. J. (2011). Visualising gold inside tumour cells following treatment with an antitumour gold(I) complex. *Metallomics*, 3(9), 917–925.
- Wiechert, W., & Noh, K. (2013). Isotopically non-stationary metabolic flux analysis: Complex yet highly informative. *Current Opinion in Biotechnology*, 24(6), 979–986.
- Winkler, B. S. (1981). Glycolytic and oxidative metabolism in relation to retinal function. *The Journal of General Physiology*, 77(6), 667–692.